Electrochimica Acta 67 (2012) 140–146

Contents lists available at SciVerse ScienceDirect

Electrochimica Acta

journal homepage: www.elsevier.com/locate/electacta

Direct electrochemistry of glucose oxidase immobilized on nanostructured gold thin films and its application to bioelectrochemical glucose sensor

Cuicui Qiu [a], Xia Wang [b], Xueying Liu [b], Shifeng Hou [c], Houyi Ma [a,*]

[a] Key Laboratory for Colloid and Interface Chemistry of State Education Ministry, School of Chemistry and Chemical Engineering, Shandong University, Jinan 250100, China
[b] State Key Laboratory of Microbial Technology, Shandong University, Jinan 250100, China
[c] Department of Chemistry and Biochemistry, Montclair State University, Montclair, NJ 07043, USA

ARTICLE INFO

Article history:
Received 9 November 2011
Received in revised form 30 January 2012
Accepted 5 February 2012
Available online 13 February 2012

Keywords:
Glucose oxidase (GOx)
Electron transfer
Bioelectrochemical sensor
Gold film
Electrochemical detection

ABSTRACT

Glucose oxidase (GOx) was stably immobilized via a simple physical adsorption method onto the nanostructured Au thin films fabricated by using electrodeposition and galvanic replacement technology, which provides a facile method to prepare morphology-controllable Au films and also facilitates the preparation and application of enzyme modified electrodes. An obvious advantage of the as-prepared enzyme electrode (denoted as GOx/Au/GCE) is that the nano-Au films provide a favorable microenvironment for GOx and facilitate the electron transfer between the active center of GOx and electrodes. Cyclic voltammetry (CV) results indicate that the immobilized GOx displayed a direct, reversible and surface-confined redox reaction in the phosphate buffer solution. Furthermore, the enzyme modified electrode was used as a glucose bioelectrochemical sensor, exhibiting a linear relationship in the concentration ranges of 2.5–32.5 $\mu mol\,L^{-1}$ and 60–130 $\mu mol\,L^{-1}$ with a detection limit of 0.32 $\mu mol\,L^{-1}$ (S/N = 3) at an applied potential of −0.55 V. Due to the excellent stability, sensitivity and anti-interference ability, the Au thin films are hopeful in the construction of glucose biosensors.

1. Introduction

With its intrinsic advantage in high sensitivity and selectivity, fast response, easy operation, and continuous on-line detection, bioelectrochemical sensors have received increasing attention in clinical medicine, biochemistry and environmental monitoring. Because of the high catalytic activity for the oxidation of glucose to gluconolactone, glucose oxidase (GOx) has been extensively used in various fields including food and beverage additives, biofuel cells, textile industry, etc. [1,2]. In particular, glucose biosensors, widely used in the direct determination of glucose in biological systems such as blood [3] and brain [4], are becoming an indispensable means for the diagnosis and therapy of diabetes mellitus.

In view of excellent selectivity and simple devices, much attention has been focused on the construction of the third generation sensor. One of the key technical problems in designing this kind of electrochemical sensors is how to achieve the fast direct electron transfer between the electrode surface and the redox active sites of the enzyme [5]. At the present time, various nanomaterials (e.g. Au [6], Pt [7], ZnO [8,9] and various carbon materials [10–14]) are used to investigate the direct electron transfer between redox enzymes and electrodes. Some technological problems, such as denaturation and leaching of immobilized enzyme, and especially long-distance electron transfer between the active sites of enzyme and the support electrodes [15–17], need to be solved urgently in developing the third generation sensor. Nowadays, the use of nanomaterials has significantly improved the performance of the biosensors and broadened their application range, which in turn greatly accelerates the development of new microminiaturized sensors. The metal-based nano-materials like Au [18,19], Pt [20,21] and Pd [22] have been widely used in building biological functional interfaces. It should be noted that, the excellent biocompatibility and interface-dominated properties of gold nanostructures have stimulated an increasing interest in designing novel and high-performance electrochemical biosensing devices [23].

In order to prepare morphology-controllable Au thin films, the nano-structured Co thin films deposited by cyclic voltammetry (CV) were used as sacrificial templates. The advantage of the present fabrication method is that the as-prepared nano-Au films were directly deposited onto the glassy carbon electrode (GCE) surface, which provides a better and more convenient boundary for enzyme immobilization than Au nanoparticles. CV and electrochemical impedance spectroscopy (EIS) were used to study the direct redox reactions of the immobilized GOx and its inhibitory effect on non-enzyme-mediated redox reactions. Moreover, the as-prepared GOx modified electrodes displayed excellent selectivity, high catalytic

* Corresponding author. Tel.: +86 531 88364959; fax: +86 531 88564464.
E-mail address: hyma@sdu.edu.cn (H. Ma).

0013-4686/$ – see front matter © 2012 Elsevier Ltd. All rights reserved.
doi:10.1016/j.electacta.2012.02.011

activity and good stability for the glucose oxidation. The obtained results are helpful for the development of high-performance glucose biosensors.

2. Experimental

2.1. Reagents and materials

Glucose oxidase (GOx, EC 1.1.3.4, 250 KU g^{-1}) was purchased from Sigma–Aldrich Co. The chemical reagents were analytical grade and the aqueous solutions were prepared with ultrapure water (>18 MΩ cm). The phosphate buffer solution (PBS, pH 6.8) was prepared by mixing NaH_2PO_4 and Na_2HPO_4 solutions. The glucose solution was left at 4 °C overnight to allow the equilibration of the optical isomerism.

2.2. Preparation of Au film modified electrode

Glassy carbon electrodes (GCEs) were ground with emery papers of decreasing particle sizes to no. 3500 finish at first, and then polished with 0.05 μm alumina slurry. Before use, the electrodes were cleaned ultrasonically in HNO_3 (1:1), washed with ultrapure water, and finally rinsed with absolute ethanol.

The Co film modified GCE (Co/GCE) was prepared following the previous procedure [24]. In a typical case, the nanostructured Co thin films were directly formed on a clean GCE (Φ = 5 mm) with continuous potential scanning at a rate of 50 mV s^{-1} between −0.95 and −0.60 V (vs. SCE) for 20 cycles in a mixture solution of 0.1 mol L^{-1} Na_2SO_4 + 10 mmol L^{-1} $Co(CH_3COO)_2$. The GCE covered with Co thin films was then immersed into 25 mmol L^{-1} $HAuCl_4$ solution for 30 min, allowing complete replacement of Co by Au. After thoroughly rinsing with ultrapure water, the Au film modified GCE (Au/GCE) was immersed in 0.1 mol L^{-1} PBS for carrying out the continuous potential cycling in the designated potential range until it gave steady CV curves. The current density in this paper was normalized by the apparent area of the electrode.

2.3. GOx immobilization

The GOx solution (2000 U mL^{-1}) was prepared with ultrapure water and stored in refrigerator at 4 °C. The freshly prepared Au/GCE was rinsed and then immersed immediately in 2000, 500, 300 U mL^{-1} GOx solutions, followed by CV cycles in PBS. After 24 h immobilization, the GOx modified Au tin film electrode (GOx/Au/GCE) was ready, then rinsed and stored in refrigerator at 4 °C for use.

2.4. Apparatus and measurements

Surface morphologies of metal thin films were observed by field emission scanning electron microscope (FESEM, Hitachi S-4800), and EDS analyses were performed with an INCAX-sight energy dispersive X-ray spectrometer equipped on the FESEM.

All electrochemical measurements were performed in a conventional three-electrode cell at room temperature (~15 °C). The modified GCE was selected as the working electrode. A bright Pt plate (1.0 cm × 1.0 cm) and a saturated calomel electrode (SCE) served as the counter electrode and the reference electrode, respectively. In this paper, all the potentials were referred to the SCE. The reference electrode was led to the surface of the working electrode through a Luggin capillary. CV, differential pulse voltammetry (DPV) and amperometry were conducted using a CHI 650A electrochemical workstation. The amperometric response of the GOx/Au/GCE for successive addition of glucose solution to the stirred PBS was recorded at −0.55 V. The electrolyte solutions were deaerated by N_2 bubbling for 10 min prior to electrochemical measurements and a blanket of N_2 was maintained throughout each experiment.

EIS was used to study the redox behavior of the p-benzoquinone/hydroquinone (BQ/HQ) couple at Au/GCE and GOx/Au/GCE electrodes. EIS measurements were carried out using EG&G potentiostat/galvanostat (Model PARC 273) and the data acquisition was performed with EG&G Powersine™. All impedance measurements were performed at 0 V (vs. open circuit potentials) in the frequency range from 10 kHz to 20 mHz using a 5 mV alternating voltage superimposed on DC potentials.

3. Results and discussion

3.1. Preparation and characterization of Au thin films

The nanostructured Co thin film was directly deposited onto a clean GCE with continuous potential sweep, and its surface morphology was shown in the inset of Fig. 1(a). The EDS spectrum shown in Fig. 1(a) gave a direct evidence for the existence of Co on the GCE substrate. The formation of Co thin films has been described in detail in the previous reports [24,25]. The nano/submicron structured Au thin films can be fabricated on the GCE substrate with ease by means of galvanic replacement of the Co films by Au(III) ions. As can be seen in Fig. 1(b), a number of Au "islands" with sizes ranging from nanometer to submicron seem to float on a loose and porous bottom layer constructed by a large quantity of Au nanoparticles (Fig. 1(c)). The high conductive, porous and biocompatible microenvironment of Au films are very suitable for enzyme immobilization, which acts as a bridge to link the active site of enzyme and the underlying electrode, not only favoring the direct electron transfer at the interface but also enhancing the stability of the enzyme modified electrode. EDS analysis of the Au films (Fig. 1(d)) only gives the signals of Au element, proving that all Co particles of different sizes were completely etched away during the galvanic replacement reaction.

3.2. Electrochemical behavior of the GOx modified electrode

3.2.1. Inhibitory effect of the immobilized GOx on non-enzymatic redox reactions

The effect of enzyme immobilization on the electron transfer in non-enzymatic redox reactions was investigated by means of CV and EIS methods. Fig. 2(a) shows the cyclic voltammograms (CVs) for Au/GCE and GOx/Au/GCE in the presence of BQ. The great difference between the two CV curves indicates that the GOx immobilization on the Au thin films has a strong inhibitory influence on the redox behavior of the BQ/HQ couple. Theoretically, the redox reaction of the BQ/HQ couple is a non-enzymatic redox reaction and can only occur at uncovered sites on the enzyme-modified electrode. The less the potential difference between oxidation and reduction peaks ($\Delta E_p = E_{pa} - E_{pc}$), the better the reversibility of redox reaction. It is observed from Fig. 2(a) that ΔE_p of the unmodified and modified electrodes were 64 mV and 320 mV, respectively. The greatly diminished current response and obviously enlarged ΔE_p after the GOx immobilization indicated that the rate of electron transfer was limited at the electrode/electrolyte interface, which resulted from the retarding of interfacial electron transfer kinetics [26,27]. In other words, the immobilized GOx behaves as a barrier layer to block the electron transfer involved in the redox process of the BQ/HQ couple.

Considering that EIS is an effective tool for probing the interfacial charge transfer on surface modified electrodes [28], the effect of enzyme concentrations on electron transfer at the enzyme modified electrodes was also investigated by means of EIS method.

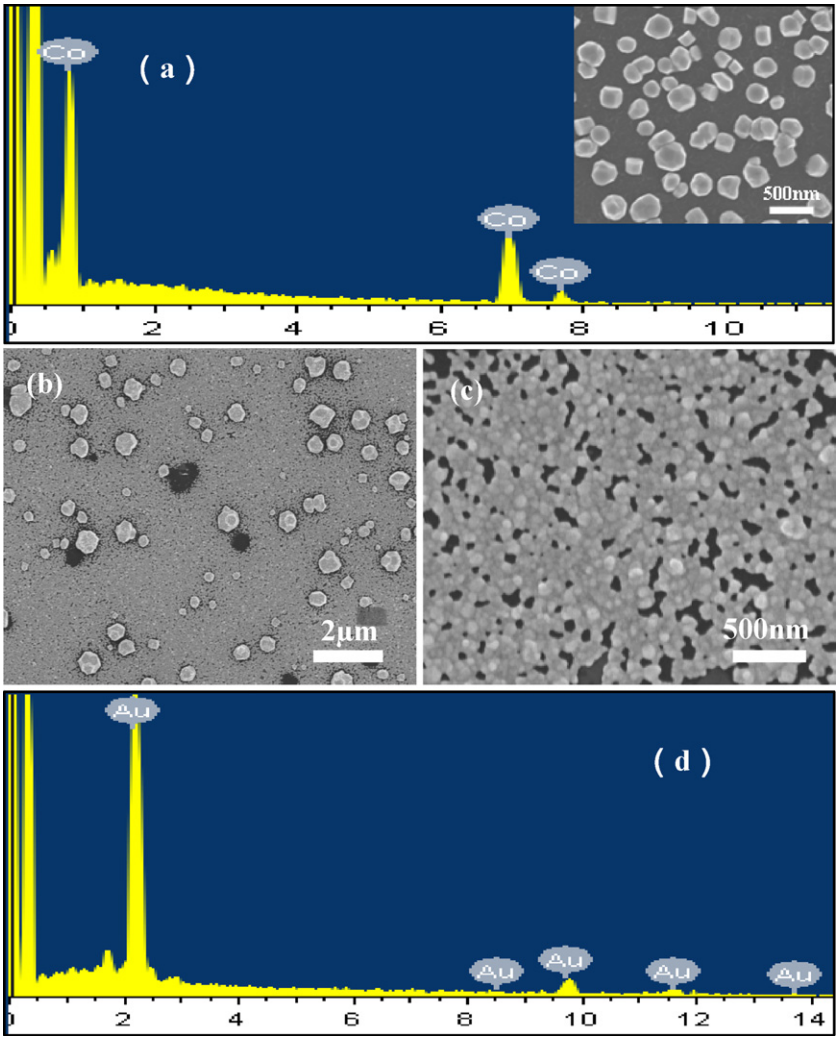

Fig. 1. EDS of Co thin film (a) and Au film (d), and SEM images of Co thin film (inset in (a)) and Au films (b, c).

Fig. 2(b) shows a set of Nyquist impedance spectra obtained with Au/GCE and GOx/Au/GCE electrodes. For the bare Au/GCE, the corresponding Nyquist spectrum displays a small depressed capacitive loop in the high frequency range (R_{ct} = 586 Ω cm^2) followed by a straight line in the low frequency region. The capacitive loop is associated with the electron transfer at the electrode/electrolyte interface, whereas the straight line in the low frequency is due to the diffusion of BQ (or HQ) from the bulk solution to the electrode surface. The diameter of the capacitive loop gradually increased but the straight line in the low frequency gradually became insignificant and finally disappeared with increasing the enzyme concentration.

The impedance spectra were fitted with the equivalent circuit shown in Table 1, and the values of circuit elements were determined and also listed in Table 1. Herein we only focus on the changes of the high frequency capacitive loops. The capacitive loop is usually related to the relaxation time constant of the charge-transfer resistance (R_{ct}) and the double-layer capacitance (CPE_{dl}) at the electrode/solution interface. The smaller the R_{ct}, the faster the rate of an electrochemical reaction [29–31]. Based on the impedance spectra measured under different conditions, there is no doubt that the immobilization of GOx on the Au thin films made the electron transfer become slow. The higher the concentrations of GOx, the more the GOx immobilized at the Au/GCE, which in turn retards more effectively the redox reaction of the BQ/HQ couple. When the concentrations of GOx increased to 2000 U mL^{-1}, the barrier layers were so dense that the diffusion process of electrochemical active species was completely blocked, which is exemplified by the disappearance of the Warburg impedance.

3.2.2. Direct electrochemistry of GOx/Au/GCE

As mentioned above, the immobilization of GOx will retard the electron transfer of non-enzyme mediated redox reactions at the electrode/solution interface; however, the direct electrochemical behavior is one of the most important features of enzyme electrodes. The cyclic voltammograms CVs of Au/GCE, GCE modified with GOx (GOx/GCE) and GOx/Au/GCE in 0.1 mol L^{-1} deaerated PBS are shown in Fig. 3(a). No obvious redox peak is observed from the CVs of the Au/GCE and only small redox peaks are found from that of the GOx/GCE. In contrast, a pair of well-defined and quasi-reversible redox peaks appear in the CVs of the GOx/Au/GCE, which should be attributed to the direct electron transfer involved in the redox process of GOx coenzyme FAD/$FADH_2$ (GOx-FAD + 2e$^-$ + 2H$^+$ ↔ GOx-$FADH_2$) [11,32]. The CVs of the GOx/Au/GCE exhibit an anodic peak at −0.434 V and a cathodic peak at −0.454 V with a small peak potential separation (ΔE_p = 20 mV) at scan rate of 50 mV s^{-1}. It is obvious that the as-prepared Au thin films provide an excellent microenvironment for GOx and significantly enhance the rate of electron transfer. It is determined that the formal potential (defined as ($E_{pa} + E_{pc}$)/2) is about −0.444 V, which is close to the standard electrode potential of FAD/$FADH_2$ at pH 7.0 (25 °C) [33].

Table 1
Equivalent circuit[a] used to fit Nyquist spectra shown in Fig. 2b and the obtained values of equivalent circuit elements.

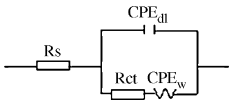

	R_s (Ω cm^2)	R_{ct} (Ω cm^2)	CPE_{dl} (Ω^{-1} cm^{-2} s^n)	CPE_W (Ω^{-1} cm^{-2} s^n)
0 U mL^{-1}	13.6	5.86×10^2	5.37×10^{-5} (n = 0.90)	1.00×10^{-2} (n = 0.45)
300 U mL^{-1}	9.29	1.07×10^3	1.17×10^{-4} (n = 0.85)	–
500 U mL^{-1}	8.06	1.50×10^3	8.37×10^{-5} (n = 0.88)	–
2000 U mL^{-1}	13.1	2.33×10^3	2.02×10^{-4} (n = 0.74)	–

[a] In the equivalent circuit, R_s, R_{ct}, CPE_{dl}, CPE_W are the solution resistance, the charge transfer resistance, the double-layer capacitance and Warburg impedance, respectively.

Fig. 3(b) shows a group of CVs for the GOx/Au/GCE at different scan rates in 0.1 mol L^{-1} deaerated PBS. It is clear that the redox peak currents are dependent on the scan rate. Moreover, there is a linear relationship between the peak current and the scan rate from 5 mV s^{-1} to 1000 mV s^{-1}. Besides, the ratio of the cathodic peak current and the anodic one (I_{pc}/I_{pa}) approximates to 1 and the formal potential keeps almost unchanged. These typical characteristics confirm that the redox reaction taking place on the GOx/Au/GCE is a surface-controlled reaction process [9–11].

According to Laviron's study [34], the adsorbance of GOx on the Au thin films can also be investigated by voltammetric method. The peak current density can be expressed as follows:

$$I_p = \frac{n^2F^2\nu A\Gamma^*}{4RT} = \frac{nFQ\nu}{4RT} \quad (1)$$

where n is electron transfer number, ν is scan rate, A is surface area of the GCE, Γ^* is the average surface concentration of GOx, Q is integral charge of the cathodic peak, T, R and F are temperature, gas constant and Faraday constant, respectively. On the basis of Eq. (1), n is determined to be 1.44, implying that two electrons are involved the redox reaction. The average surface concentration of the electroactive GOx adsorbed on the Au/GCE is calculated to be 2.58×10^{-10} mol cm^{-2} from the slope of the I_p–ν curve. This value is larger than the literature value (1.27×10^{-10} mol cm^{-2}) [35], thereby suggesting that the Au films provide a large area for the enzyme immobilization.

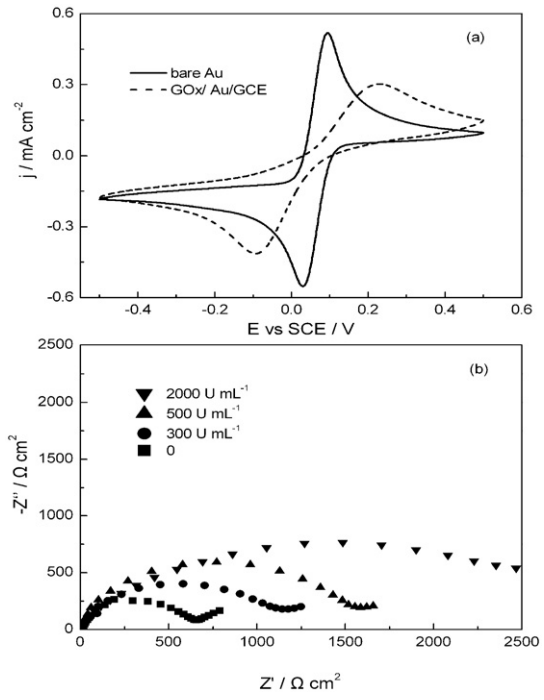

Fig. 2. (a) CVs of the Au/GCE and GOx/Au/GCE in 0.1 mol L^{-1} PBS +5 mmol L^{-1} BQ mixed solutions. Scan rate: 50 mV s^{-1}. GOx concentration: 2000 U mL^{-1}. (b) Nyquist impedance spectra for GOx/Au/GCE with different concentrations of GOx in 0.1 mol L^{-1} PBS + 5 mmol L^{-1} BQ mixed solutions at 0 V with respect to open circuit potentials.

3.3. Electrochemical detection of glucose

3.3.1. Electrochemical behavior of GOx/Au/GCE in the presence of glucose

The CVs in Fig. 4(a) show the effect of glucose concentrations on the electrochemical behavior of GOx/Au/GCE. As the glucose concentration increased, the redox peak current of FAD/FADH$_2$ was observed to decrease obviously, which has been reported previously [36,37]. In order to have a better understanding of the electrochemical behavior of the GOx/Au/GCE in the presence of glucose, the voltammetric behavior of three different electrodes, Au/GCE, GOx/GCE and Au/GCE modified with inactivated GOx (inactivated-GOx/Au/GCE), were investigated under identical conditions and the CVs recorded were shown in Fig. 4(b) for

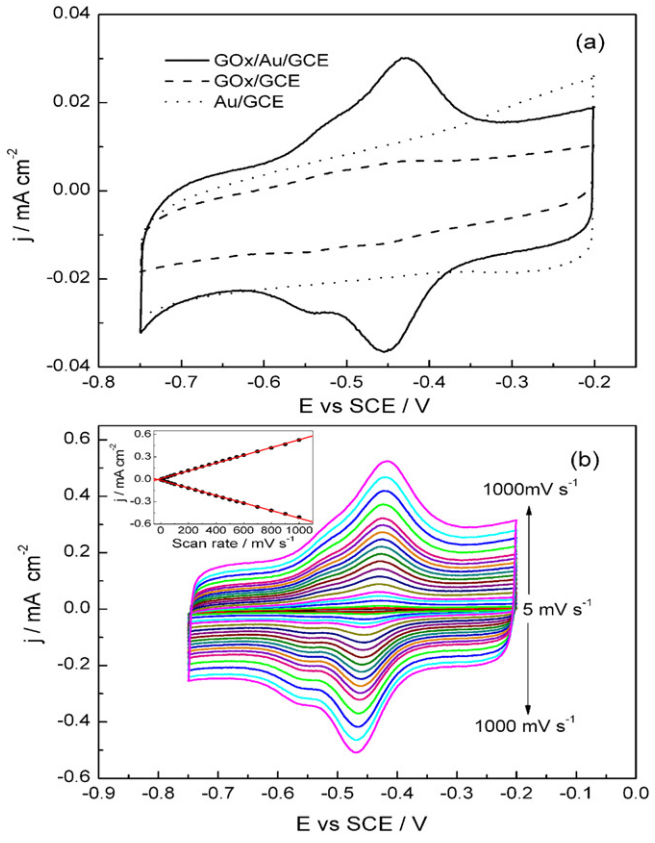

Fig. 3. (a) CVs of Au/GCE, GOx/GCE and GOx/Au/GCE in 0.1 mol L^{-1} PBS (scan rate: 50 mV s^{-1}); (b) CVs of GOx/Au/GCE measured at scan rates of 5, 10, 20, 50, 75, 100, 150, 200, 250, 300, 350, 400, 450, 500, 550, 600, 700, 800, 900, 1000 mV s^{-1} in 0.1 mol L^{-1} PBS.

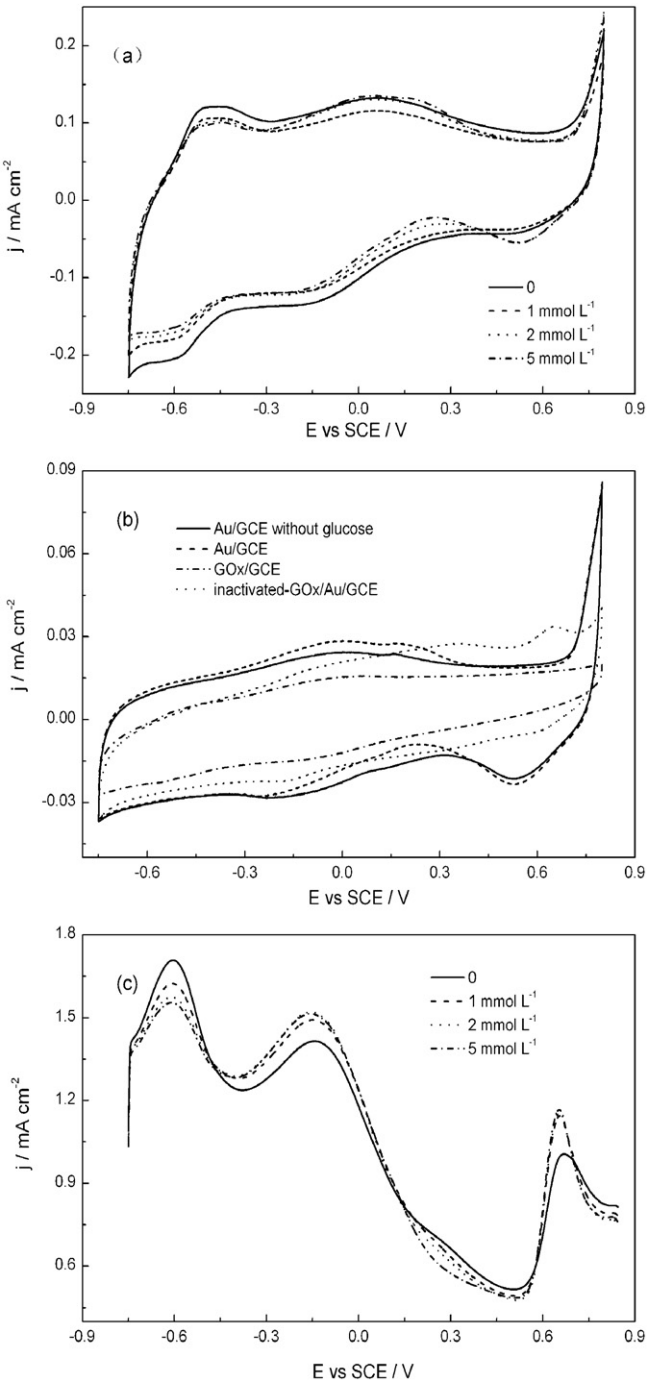

Fig. 4. (a) CVs of GOx/Au/GCE in 0.1 mol L^{-1} PBS with different concentrations of glucose (scan rate: 50 mV s^{-1}); (b) CVs of Au/GCE, GOx/GCE and inactivated-GOx/Au/GCE in mixed solutions of 0.1 mol L^{-1} PBS and 1 mmol L^{-1} glucose at a scan rate of 50 mV s^{-1}; (c) difference pulse voltammograms of GOx/Au/GCE in 0.1 mol L^{-1} PBS with different concentrations of glucose.

comparison. It was found from Fig. 4(b) that, in the absence of glucose, the Au/GCE electrode started to be oxidized at ~0.65 V in the positive-going potential scan, leading to a sharp increase in current density; the reduction of Au oxides took place at ~0.53 V during the negative-going potential scan, producing a broad cathodic peak. However, a notable increase in current appeared at ~0.25 V in the presence of glucose, as can be seen from the dashed curve. By comparing the CVs of Au/GCE and GOx/Au/GCE under identical conditions, it is concluded that that the immobilization of GOx significantly inhibited the oxidation of Au films since gold oxide reduction peak almost disappeared during the negative-going potential scan (see Fig. 4(a)). Furthermore, the electrooxidation of glucose on Au sites was also inhibited on the GOx/Au/GCE. Fig. 4(b) has clearly shown that no obvious electrooxidation of glucose took place on both the GOx/GCE and inactivated-GOx/Au/GCE. Nevertheless, the redox peaks of FAD/$FADH_2$ decreased for GOx/GCE (compared with the CV curve in Fig. 3(a) in the absence of glucose) and disappeared for inactivated-GOx/Au/GCE (compared with the CV curve of GOx/Au/GCE).

The decrease of redox peak current of FAD/$FADH_2$ was also demonstrated by the results of DPV (shown in Fig. 4(c)). Each DPV curve displays three well-defined oxidation peaks in the potential range between −0.8 and 0.8 V. The peaks at ~−0.15 V and ~0.66 V are derived from the redox reaction of glassy carbon and Au, respectively. The peak at ~−0.6 V is attributed to the redox process of FAD/$FADH_2$, which significantly decreased with the increase of glucose concentration. The results indicate that the addition of glucose produces a significant influence on the direct electron transfer of GOx, which in turn provides a feasible path to detect the changes of glucose concentration.

3.4. Amperometric detection of glucose

It is well-known that GOx possesses a high-efficiency catalytic activity toward glucose oxidation. The reaction between glucose and GOx in the presence of oxygen can be described by Eqs. (2) and (3) [38,39]:

$$GOx_{ox} + \beta\text{-d(+)-glucose} \rightarrow GOx_{red} + \text{d-gluconicacid} \quad (2)$$

$$GOx_{red} + O_2 \rightarrow GOx_{ox} + H_2O_2 \quad (3)$$

where the dissolved molecular oxygen acts as an electron acceptor.

Fig. 5(a) shows a typical current-time curve of the glucose biosensor based on the GOx/Au/GCE at an applied constant potential of −0.55 V. A well-defined and fast amperometric response was observed at the potential. The detection range of glucose was from 2.5 μmol L^{-1} to 157.5 μmol L^{-1}. The inset shown in the upper right of Fig. 5(a) presents calibration curves for steady state current versus glucose concentrations. Two linear ranges were obtained and the fitting regression equations were given as follows:

$$I = -2.11 - 0.074C(2.5 - 32.5\ \mu\text{mol L}^{-1},\ R = 0.998,\ n = 14) \quad (4)$$

$$I = -4.44 - 0.011C(60 - 130\ \mu\text{mol L}^{-1},\ R = 0.997,\ n = 29) \quad (5)$$

The limit of detection is 0.32 μmol L^{-1} (S/N = 3). When the concentration of glucose further increased to more than 150 μmol L^{-1}, the current response tended to become a plateau, which is the typical characteristic of the Michaelis–Menten kinetics. The apparent Michaelis–Menten constant (k_m), which gives an indication of the enzyme-substrate kinetics for the biosensor, can be calculated using the Lineweaver–Burk equation [40]:

$$\frac{1}{i_s} = \frac{k_m}{i_{max}}\frac{1}{C} + \frac{1}{i_{max}} \quad (6)$$

where i_s is the steady-state current, C is the concentration of glucose, k_m is the apparent Michaelis–Menten constant, and i_{max} is the maximum current. From the curve of the i_s^{-1} vs C^{-1}, the k_m is estimated to be 15.6 μmol L^{-1} and the i_{max} is 6.5 μA. In order to identify the role of GOx in the determination of glucose, the amperometric responses of Au/GCE, GOx/GCE and inactivated-GOx/Au/GCE caused by successive addition of 2.5 μmol L^{-1} glucose to the stirred 0.1 mol L^{-1} PBS are shown in Fig. 5(b). It was observed that, though a current step was caused by the addition of glucose, no steady current produced and no linear relationship between glucose concentration and current response were obtained on Au/GCE. For the inactivated-GOx/Au/GCE, no distinct

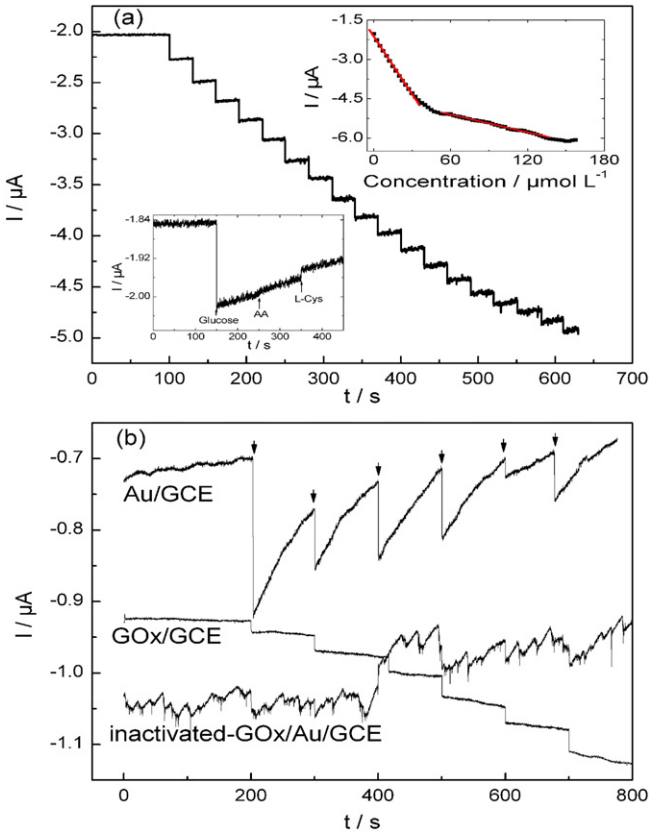

Fig. 5. (a) Typical steady-state response of the as-prepared GOx/Au/GCE for successive concentration increments of 2.5 μmol L^{-1} glucose in stirred 0.1 mol L^{-1} PBS; (b) current response of Au/GCE, GOx/GCE and inactivated-GOx/Au/GCE for successive addition of 2.5 μmol L^{-1} glucose to the stirred 0.1 mol L^{-1} PBS. Applied potential: −0.55 V. Insets in the upper right and the lower left of (a) present the calibration curve and anti-interference performance of GOx/Au/GCE, respectively.

current response was observed. In contrast, regular amperometric responses were achieved on the GOx/GCE although the current step was smaller than that acquired using the GOx/Au/GCE. This fact indicates that the Au thin films have relatively larger specific surfaces for the immobilization of GOx and the immobilized GOx therefore possesses a high enzymatic activity and a good affinity toward glucose.

3.5. Stability and repeatability of enzyme modified electrode

Stability is a basic requirement for fabrication of glucose sensors. The leaching of the immobilized GOx during the usage was investigated by comparing the changes of redox peak of FAD/$FADH_2$ from their CVs measured in mixed solutions of 0.1 mol L^{-1} PBS and 0.1 mmol L^{-1} glucose. In the initial period, the oxidation peak current was observed to gradually increase with the number of CV cycles and reach the maximum in the 50th cycle (20% larger than the initial current). As the voltammetric cycling went on, the peak current slowly decreased. For example, the peak current in the 300th cycle was 107% of the initial value and 89.3% of the maximum. These results clearly indicated that the immobilized GOx was difficult to leach from the Au thin film, which demonstrated that the GOx modified electrode exhibited the excellent stability and reusability.

At the same time, the storage stability of the GOx modified electrode was also investigated. The as-prepared enzyme electrode was preserved in ultra-pure water at 4 °C in refrigerator. The slight decrease in the sensitivity during the first 7 days (about 94.6% of remains) was caused primarily by the leaching of the bound enzyme from the electrode surface [41]. In the next few weeks, the rate of decay for enzyme response was significantly reduced. 35 days after being stored, the current response of GOx was 87.5% of its initial value. The long-time stability test shows that 85.3% of enzyme activity was still retained after 70 days. This suggests that the GOx/Au/GCE is quite efficient for retaining the activity of GOx. The good stability may be attributed to the excellent biocompatibility of Au nanostructures, which provided a favorable microenvironment for GOx to retain its bioactivity and strong adsorption on the Au film.

The repeatability of GOx/Au/GCE was also investigated by detecting the response to 2.5 μmol L^{-1} glucose for five consecutive measurements. The relative standard deviation (RSD) was 3.5%, indicating that the biosensor had good repeatability.

3.6. Specificity and Interferences

It is well-known that enzyme is highly specific for substrate. The selectivity of the enzyme electrode is closely related to the property of enzyme. The GOx possesses the high specific catalytic activity toward the glucose oxidation even though in the presence of other carbohydrates. The main interferences of enzyme sensors are caused by the electroactive species diffusing to the sensor surface.

In this work, 2.5 μmol L^{-1} ascorbic acid (AA) and cysteine (L-Cys) were consecutively added into the mixed solution of 0.1 mol L^{-1} PBS and 2.5 μmol L^{-1} glucose to study the anti-interference performance of GOx/Au/GCE in the amperometric detection process. As can be seen from the inset in the lower left of Fig. 5(a), the addition of AA caused no obvious current response. However, 9.7% current increment was observed when L-Cys was added. Considering that the concentration of L-Cys in human serum is much smaller than that of glucose (normal range: 4–7 mmol L^{-1}), in fact the presence of L-Cys hardly affected the detection of glucose in serum samples. Besides, the anti-interference of the enzyme modified electrode was further tested by DPV. The addition of 5 mmol L^{-1} glucose causes a decrease of the peak current at ~−0.6 V. However, the current peak almost remained unchanged when 5 mmol L^{-1} α-sucrose, D-fructose, D-mannose and D-xylose were added to the mixed solution of PBS and glucose. All the results imply that the as-prepared biosensor has excellent anti-interference ability. This is the reason why we immobilized GOx on electrode surface in the detection of glucose.

3.7. Determination of glucose in human serum sample

The GOx/Au/GCE was applied to the determination of glucose concentration in human serum. A rapid and stable amperometric response was acquired at −0.55 V with the direct addition of 20 μL of samples into 20 mL of 0.1 mol L^{-1} PBS. The content of glucose in the samples was calculated from the calibration curve and the obtained results were shown in Table 2. Herein the concentration of glucose in the sample was also measured using a blood sugar analyzer (SBA-40C). The values given by the analyzer were in good agreement with our results, thereby demonstrating that the

Table 2
The comparison between the concentration values of glucose measured with GOx/Au/GCE biosensor and SBA-40C blood sugar analyzer (average values of 4 measurements).

Sample no.	Concentrations of glucose (mmol L^{-1})		Deviation (mmol L^{-1})
	Determined by GOx modified electrode	Determined by blood sugar–glucose analyzer	
1	7.04	7.105	−0.065
2	6.70	6.55	+0.15

as-prepared biosensor was effective and sensitive for the determination of glucose in actual samples.

4. Conclusions

Nano/submicron structured Au films were fabricated onto GCEs using nanostructured Co thin films as the sacrificial templates to react with $HAuCl_4$. The as-prepared Au thin films provide an excellent microenvironment for the adsorption of GOx. The immobilized GOx displays strong inhibition effect on the electron transfer of non-enzyme-mediated redox reactions but presents good catalytic activity and selectivity for the glucose oxidation. Because of the excellent sensing performance with high sensitivity, anti-interference ability and good stability, the GOx/Au/GCE is expected to act as premising biosensors for the selective detection of glucose.

Acknowledgment

This work was supported by National Natural Science Foundation of China (21073111, 21175059) and National Basic Research Program of China (2009CB930103).

References

[1] C.M. Wong, K.H. Wong, X.D. Chen, Appl. Microbiol. Biotechnol. 78 (2008) 927.
[2] S.B. Bankar, M.V. Bule, R.S. Singhal, L. Ananthanarayan, Biotechnol. Adv. 27 (2009) 489.
[3] M.E. Sangill, B. Pedersen, Am. J. Kidney Dis. 47 (2006) 636.
[4] F. Ahmad, A.P. Md Yusof, M. Bainbridge, S. Ab Ghani, Biosens. Bioelectron. 23 (2008) 1862.
[5] S. Park, H. Boo, T.D. Chung, Anal. Chim. Acta 556 (2006) 46.
[6] J. Li, J. Yu, F. Zhao, B. Zeng, Anal. Chim. Acta 587 (2007) 33.
[7] Y. Wang, R. Yuan, Y. Chai, W. Li, Y. Zhuo, Y. Yuan, J. Li, J. Mol. Catal. B: Enzym. 71 (2011) 146.
[8] Y. Zhai, S. Zhai, G. Chen, K. Zhang, Q. Yue, L. Wang, J. Liu, J. Jia, J. Electroanal. Chem. 656 (2011) 198.
[9] F. Hu, S. Chen, C. Wang, R. Yuan, Y. Chai, Y. Xiang, C. Wang, J. Mol. Catal. B: Enzym. 72 (2011) 298.
[10] M. Li, S. Xu, M. Tang, L. Liu, F. Gao, Y. Wang, Electrochim. Acta 56 (2011) 1144.
[11] Q. Liu, X. Lu, J. Li, X. Yao, J. Li, Biosens. Bioelectron. 22 (2007) 3203.
[12] Y. Shao, J. Wang, H. Wu, J. Liu, I.A. Aksay, Y. Lin, Electroanalysis 22 (2010) 1027.
[13] C. Deng, J. Chen, X. Chen, C. Xiao, L. Nie, S. Yao, Biosens. Bioelectron. 23 (2008) 1272.
[14] X. Shangguan, H. Zhang, J. Zheng, Electrochem. Commun. 10 (2008) 1140.
[15] Z. Cao, Y. Zou, C. Xiang, L.-X. Sun, F. Xu, Anal. Lett. 40 (2007) 2116.
[16] Y. Huang, W. Zhang, H. Xiao, G. Li, Biosens. Bioelectron. 21 (2005) 817.
[17] Z.H. Dai, J. Ni, X.H. Huang, G.F. Lu, J.C. Bao, Bioelectrochemistry 70 (2007) 250.
[18] D. Feng, F. Wang, Z. Chen, Sens. Actuators B 138 (2009) 539.
[19] O. Yehezkeli, Y.-M. Yan, I. Baravik, R. Tel-Vered, I. Willner, Chem. Eur. J. 15 (2009) 2674.
[20] X. Chu, D. Duan, G. Shen, R. Yu, Talanta 71 (2007) 2040.
[21] Z. Wen, S. Ci, J. Li, J. Phys. Chem. C 113 (2009) 13482.
[22] C.-H. Lee, S.-C. Wang, C.-J. Yuan, M.-F. Wen, K.-S. Chang, Biosens. Bioelectron. 22 (2007) 877.
[23] Y. Li, H.J. Schluesener, S. Xu, Gold Bull. 43 (2010) 29.
[24] J.T. Zhang, C.C. Qiu, H.Y. Ma, X.Y. Liu, J. Phys. Chem. C 112 (2008) 13970.
[25] Q.S. Chen, S.G. Sun, J.W. Yan, J.T. Li, Z.Y. Zhou, Langmuir 22 (2006) 10575.
[26] S. Zhang, N. Wang, Y. Niu, C. Sun, Sens. Actuators B 109 (2005) 367.
[27] R.K. Shervedani, A.H. Mehrjardi, N. Zamiri, Bioelectrochemistry 69 (2006) 201.
[28] F. Patolsky, M. Zayats, E. Katz, I. Willner, Anal. Chem. 71 (1999) 3171.
[29] H.Y. Ma, C. Yang, S.H. Chen, Y.L. Jiao, S.X. Huang, D.G. Li, J.L. Luo, Electrochim. Acta 48 (2003) 4277.
[30] H.Y. Ma, L.-Y. Ou Yang, N. Pan, S.-L. Yau, J.Z. Jiang, K. Itaya, Langmuir 22 (2006) 2105.
[31] X.J. Wu, H.Y. Ma, S.H. Chen, Z.Y. Xu, A.F. Sui, J. Electrochem. Soc. 146 (1999) 1847.
[32] G. Wang, N.M. Thai, S.-T. Yau, Biosens. Bioelectron. 22 (2007) 2158.
[33] I. Tinoco, K. Kauer, J.C. Wang, Physical Chemistry-Principles and Applications in Biological Sciences, Prentice-Hall, Englewood Cliffs, NJ, 1978, p. 606.
[34] E. Laviron, J. Electroanal. Chem. 100 (1979) 263.
[35] R.F. Gao, J.B. Zheng, Electrochem. Commun. 11 (2009) 608.
[36] F.H. Li, J.X. Song, F. Li, X.D. Wang, Q.X. Zhang, D.X. Han, A. Ivaska, L. Niu, Biosens. Bioelectron. 25 (2009) 883.
[37] Y.H. Wu, S.S. Hu, Bioelectrochemistry 70 (2007) 335.
[38] Q.J. Chi, S.J. Dong, Anal. Chim. Acta 278 (1993) 17.
[39] C.X. Lei, H. Wang, G.L. Shen, R.Q. Yu, Electroanalysis 16 (2004) 736.
[40] R.A. Kamin, G.S. Wilson, Anal. Chem. 52 (1980) 1198.
[41] J.H. Pei, X.-Y. Li, Electroanalysis 11 (1999) 1266.